NeuroImage 138 (2016) 211–220

Contents lists available at ScienceDirect

NeuroImage

journal homepage: www.elsevier.com/locate/ynimg

Color responses and their adaptation in human superior colliculus and lateral geniculate nucleus

Dorita H.F. Chang [1], Robert F. Hess, Kathy T. Mullen *

McGill Vision Research, Department of Ophthalmology, McGill University, Canada

ARTICLE INFO

Article history:
Received 20 April 2016
Accepted 26 April 2016
Available online 3 May 2016

Keywords:
fMRI adaptation
L/M-cone opponent
LGN
SC

ABSTRACT

We use an fMRI adaptation paradigm to explore the selectivity of human responses in the lateral geniculate nucleus (LGN) and superior colliculus (SC) to red–green color and achromatic contrast. We measured responses to red–green (RG) and achromatic (ACH) high contrast sinewave counter-phasing rings with and without adaptation, within a block design. The signal for the RG test stimulus was reduced following both RG and ACH adaptation, whereas the signal for the ACH test was unaffected by either adaptor. These results provide compelling evidence that the human LGN and SC have significant capacity for color adaptation. Since in the LGN red–green responses are mediated by P cells, these findings are in contrast to earlier neurophysiological data from non-human primates that have shown weak or no contrast adaptation in the P pathway. Cross-adaptation of the red–green color response by achromatic contrast suggests unselective response adaptation and points to a dual role for P cells in responding to both color and achromatic contrast. We further show that subcortical adaptation is not restricted to the geniculostriate system, but is also present in the superior colliculus (SC), an oculomotor region that until recently, has been thought to be color-blind. Our data show that the human SC not only responds to red–green color contrast, but like the LGN, shows reliable but unselective adaptation.

Introduction

Viewing a stimulus for an extended period may result in a change in its perceived appearance when viewed again subsequently (Blakemore & Campbell, 1969). This phenomenon, referred to as perceptual (contrast) adaptation, has been used to study the specificity of neural mechanisms to particular visual attributes by examining how effects transfer across stimuli. As adaptation effects have been repeatedly shown to be orientation-specific, it has been widely assumed that the underlying mechanisms must emerge at the cortical, rather than subcortical level. Indeed, early physiological data obtained from both the cat and the macaque have indicated significant capacity for adaptation with cortical neurons (Maffei et al., 1973; Movshon & Lennie, 1979; Ohzawa et al., 1985; Sclar et al., 1989; Carandini et al., 1998), in contrast to the lack of adaptation in the subcortical, lateral geniculate nucleus (LGN) of the geniculostriate pathway (Maffei et al., 1973; Movshon & Lennie, 1979; Derrington et al., 1984; Ohzawa et al., 1985; Shou et al., 1996). In more recent work, however, adaptation has been shown to occur as early as the retina in some primate (Chander & Chichilnisky, 2001) and non-primate species (Smirnakis et al., 1997; Kim & Rieke, 2001; Brown & Masland, 2001; Baccus & Meister, 2002), although it should be noted that the varied stimuli employed and the different species used across different studies may account, at least in part, for the seemingly discrepant data.

Nevertheless, an increasing body of literature points to adaptation mechanisms occurring early in visual processing, including the LGN (Solomon et al., 2004; Camp et al., 2009; McLelland et al., 2010). In the macaque, Solomon et al. (2004) showed that M cells in the LGN, but not P cells, show strong contrast adaptation.

Little is known about the response properties of the LGN in humans. The LGN is the primary thalamic nucleus for the neural pathway between the retina and the primary visual cortex. One important feature of the LGN is its organization: retinal inputs are segregated into different layers. The retinal parvocellular P-cells project to dorsal layers 3–6, and the magnocellular M-cells project to ventral layers 1 and 2. There are still further cell types in the intralaminar (koniocellular) layers. The LGN is a particularly interesting region to consider in the domain of color vision as these different layers offer a basis for segregation based on the chromatic properties of the cells. P-cells constitute the largest neuronal population and form the basis of red–green color vision with L/M-cone opponency and high sensitivity to RG color contrast (Derrington et al., 1984; Lee et al., 1990). In line with this, data from human fMRI of the LGN have shown strong responses to isoluminant red–green contrast that selectively activate the L/M cone opponent system (Mullen et al., 2008, 2010; Zhang et al., 2015). M-cells, by comparison, are primarily achromatic with high contrast gain at high temporal frequencies (Kaplan & Shapley, 1982; Derrington et al., 1984;

* Corresponding author at: McGill Vision Research, Department of Ophthalmology, McGill University, 1650 Ave Cedar, Montreal H3G 1A4, Canada.
E-mail address: kathy.mullen@mcgill.ca (K.T. Mullen).
[1] Present address: Department of Psychology, The University of Hong Kong, Hong Kong.

http://dx.doi.org/10.1016/j.neuroimage.2016.04.067

Derrington & Lennie, 1984; Lee et al., 1990; Solomon et al., 1999). Note that the distinction between the roles of P- and M-cells for processing achromatic contrast may not be clear cut, however, as P cells are thought to play a "double duty" role in responding not only to red–green color contrast, but also to achromatic contrast at higher spatial frequencies (Lennie & D'Zmura, 1988; Lennie et al., 1991; Merigan et al., 1991).

Here, we use an fMRI adaptation method to explore the selectivity of responses to red–green color and achromatic contrast in the human lateral geniculate nucleus (LGN). For comparison, we also consider responses in another visual subcortical structure along the retinotectal pathway, the human super colliculus (SC). The superior colliculus is a laminar structure located in the midbrain that belongs to a network of areas mediating eye movements and directed attention. The SC is roughly subdivided into a superficial part, which predominantly processes visual information, and a deeper part, which is predominantly responsible for orienting movements of the eyes and the head. In the superficial layers, neurons respond well to a broad range of transient or moving visual stimuli independent of stimulus orientation, size, shape, or movement velocity (Cynader & Berman, 1972; Schiller & Stryker, 1972; Marrocco & Li, 1977). Early physiological studies indicated that the visual SC neurons of primates are unresponsive to color signals (e.g., Marrocco & Li, 1977; Schiller & Malpeli, 1977) and thus thought to be largely achromatic. Correspondingly, the SC has been presumed to be involved in human blindsight, which psychophysically has poor or absent responses to color (Stoerig & Cowey, 1989; Cowey et al., 2003; Leh et al. 2006). More recent neurophysiological data, however, point to robust responses of the primate SC to color. In particular SC neurons seem to respond well to the P-cell targeted red–green stimulus (White et al., 2009) as well as the S-cone isolating blue–yellow stimulus (Hall & Colby, 2014; Herman & Krauzlis, 2014). Using fMRI, the human SC has also been shown to be responsive to red–green color contrast (Zhang et al., 2015). Beyond this, very little is known about the visual response properties of the SC. Indeed, the SC is difficult to study in detail with functional brain imaging techniques because of its small size, deep location, and proximity to vascular structures that cause a high degree of physiological noise in the midbrain and brain stem. Hence, this region a good candidate to examine in the human alongside the LGN for color adaptation.

In line with the logic of other adaptation techniques, fMRI adaptation assumes that BOLD signals are reduced when two successive visual stimuli stimulate the same neural population but not when they activate different populations (Engel & Furmanski, 2001; Grill-Spector & Malach, 2001; Engel, 2005; Fang et al., 2005; Krekelberg et al., 2006). That is, with this paradigm we can reveal the degree to which the responses in the human subcortical structures are *selective* to chromatic (red–green) and achromatic contrast. Using this protocol, we have previously shown a functional dissociation along the human cortex, towards achromatic selectivity in the dorsal cortex (V3a, hMT+), and chromatic (red–green) selectivity in the ventral cortex (ventral occipital cortex, VO) (Mullen et al., 2015). Here, we use fMRI adaptation to further clarify the roles of the subcortical structures in human vision, the LGN and SC.

Methods

Participants

Thirteen observers (10 females, 3 males) participated in the main experiment. Four of these participants were tested additionally in a control experiment. All observers had normal or corrected-to-normal vision, were screened for color deficiencies, and provided written informed consent in line with local ethical review and approval of the work obtained from both the Medical Research Ethics Committee of the University of Queensland for MRI experiments on humans, and the Centre for Magnetic Resonance and the McConnell Brain Imaging Centre at the Montreal Neurological Institute and Hospital. All participants were screened for fMRI contra-indications.

Apparatus

Stimuli were generated using Matlab with extensions from PsychToolbox (Brainard, 1997; Pelli, 1997) on a Macintosh computer. Images were back-projected on a screen using a LCD projector (NEC VT580, resolution 1024 × 768, frame rate = 60 Hz, mean luminance = 270 cd/m^2) that was placed at the back of the bore 1 m from the participant. For the psychophysical experiments used to determine detection threshold and isoluminance, stimuli were generated using a VSG 2/5 graphics board with 15 bits of contrast resolution (Cambridge Research Systems Ltd., Rochester, England) housed in a Pentium PC computer and displayed on a CRT monitor (Diamond Pro 2030). Both projection and CRT displays were linearized and color calibrated as previously described (Mullen et al., 2007; Michna & Mullen, 2008). The cone contrast gamut is most limited in the red–green direction, with an upper cone contrast limit for the projection system of around 5% for the RG stimuli, depending precisely on the calibration data, the projector settings, and the isoluminant point.

Stimuli

For the main experiment, both test and adapting stimuli were radial sinewave gratings (0.5 cycles/degree) with contrast sinusoidally phase reversing at 2 Hz (Mullen et al., 2007; Mullen et al., 2008), presented in a temporal Gaussian contrast envelope (sigma = 125 ms). In a subsequent control experiment, stimuli were presented at 8 Hz. Isoluminant red–green chromatic (RG) and achromatic (ACH) stimuli (also isoluminant with respect to the background) were used that isolated the L/M cone opponent and luminance (achromatic) post-receptoral mechanisms, respectively (Fig. 1). The cone contrasts of the stimuli were fixed at 4.0% or 22% for the RG and ACH conditions, respectively, in order to create highly visible suprathreshold stimuli and maximize signal strength. Contrasts were the same for test and adapting stimuli. Stimulus size was 19° (full width) by approximately 19° (full height). A small fixation dot was present in the center of the stimulus. The radial stimulus arrangement permitted a spatially narrow band stimulus to be displayed at a relatively low spatial frequency. A spatial frequency of 0.5 cycles/degree was chosen to avoid artifacts generated by chromatic aberration in the chromatic stimuli (Bradley et al., 1992; Cottaris, 2003) and to optimize chromatic contrast sensitivity (Mullen, 1985).

Stimulus chromaticity was defined using a 3-dimensional cone contrast space in which each axis represents the quantal catch of the L, M and S cone types normalized with respect to the white background (i.e. cone contrast). Chromaticity is given by the vector direction and contrast by vector length within this space. Isoluminance of the RG stimuli was determined for each subject individually, using a gabor (7°, 0.5 cpd) shown centrally, and using methods previously described (Mullen et al., 2007, 2010).

Procedure

Red–green (RG) or achromatic (ACH) adaptation runs were conducted in separate sessions on separate days, with the order of the adaptor used first (RG or ACH) counterbalanced across participants. Each run was composed of repetitions of three sequential blocks, as illustrated in Fig. 1: 1) adaptation block (12 s) comprising continuous presentation of either the adapting stimulus or a blank (no-adapt) field; 2) test block (18 s) comprising six sequential test stimulus presentations of: i. all RG stimuli, ii. all ACH stimuli, or iii. alternating RG and ACH stimuli; 3) fixation block (9 s) (further details below). Each sequence (adaptation–test–fixation) had three repetitions to allow each of the three test blocks (i–iii) to be represented, with test block order

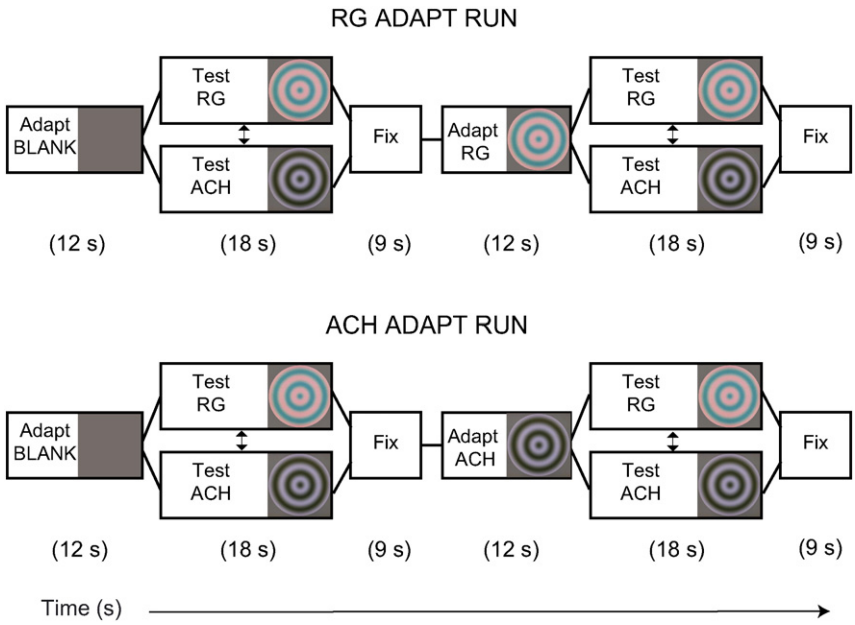

Fig. 1. Scan protocol (block-design). A particular scan run was composed of repetitions of three sequential blocks: 1. an *adaptation* block comprising repeated presentation of the adapting stimulus or a blank, no-adapt field; 2. a *test* block comprising six sequential test stimulus presentations of only RG stimuli, only Ach stimuli, or alternating RG and Ach stimuli; 3. a *fixation* block. A given sequence consisted of three repetitions of these three blocks, one for each test type, with test block order pseudo-randomized. The sequences were arranged such that the blank-adapt and stimulus-adapt sequences alternated with the starting sequence (adapt or no-adapt) chosen pseudo-randomly. Within one run, the stimulus-adaptor and blank-adaptor were each presented 9 times (3 times preceding each of the RG, ACH, and MIX tests), and each test was presented a total of 6 times (3 times following stimulus adaptation, and 3 times following blank adaptation).

pseudo-randomized. The sequences were arranged such that the blank-adapt and stimulus-adapt sequences alternated with the starting sequence (adapt or no-adapt) chosen pseudo-randomly. Within one run, the stimulus-adaptor and blank-adaptor were each presented 9 times (3 times preceding each of the RG, ACH, and MIX tests), and each test was presented a total of 6 times (3 times following stimulus adaptation, and 3 times following blank adaptation). One run lasted approximately 12 min and subjects performed a minimum of four runs per adaptor (RG or ACH). Subject data from all runs were averaged before being entered into the group-wise analyses. The mixed test condition (iii) using alternating test stimuli was inserted as part of a different experiment to test for shorter term adaptation effects produced by the repeated brief (0.5 s) exposures to the test stimuli during the 18 s test block. Since we found no difference between the BOLD responses to the mixed and all-RG or all-ACH stimuli across the time course of the stimulus block in our ROIs, we concluded that short-term, self-adaptation from the multiple test stimuli presentations was insignificant and we did not pursue this further.

The test block consisted of stimuli presented in six consecutive test trials of 3 s each, as previously described (Mullen et al., 2007). During the tests, we engaged the observer in a contrast discrimination task designed to control for attention and task demands. On each trial, observers made a two-interval two-alternative forced-choice between two intervals both displaying stimuli from the same condition (e.g. RG) but with a small, barely discernable contrast difference between them, fixed at 30% ($\pm$15% of mean) for each participant. The observer's task was to indicate the interval containing the higher contrast stimulus using a two-button response box. Participants were familiarized with the task before entering the scanner. Each stimulus was presented within a 500 ms time window in a temporal Gaussian contrast envelope (sigma = 125 ms) with an inter-stimulus interval of 500 ms. In the remaining 1.5 s, the subject's response was given by a button press. Fixation blocks consisted of a ring of the same chromaticity as the stimulus that modulated at 2 Hz and surrounded a small fixation spot.

In a control experiment, all procedures were identical to the main experiment except that stimuli (and fixation) modulated at 8 Hz. Only achromatic test stimuli were used in this experiment as we were interested in testing any variation in adaptation for ACH stimuli at a higher temporal frequency. Consequently, one particular run comprised 12 repetitions of the test block (always ACH), six following no-adaptation, and six following RG or ACH adaptation. The entire run lasted approximately 8 min.

fMRI acquisition and data analysis

fMRI data were acquired for four of the thirteen participants using a 4 T Bruker MedSpec system at the Centre for Magnetic Resonance, Brisbane, Australia, and on a 3 T Siemens TIM Trio at the McConnell Brain Imaging Centre of the Montreal Neurological Institute for the remaining eight participants and in the control experiment. A 32-channel SENSE head coil (3 T) was used for radiofrequency transmission and reception (Vaughan et al., 2002). EPI data (Gradient echo-pulse sequences) were acquired from 44 slices (whole brain coverage, TR 3000 ms, TE: 30 ms, 3.0 mm^3 resolution). Slices were oriented parallel to the calcarine sulcus. Head movement was limited by foam padding within the head coil. For each participant, a high-resolution 3D T1 image was acquired using an MP-RAGE sequence with TI 1500 ms, TR 2500 ms, TE 3.83 ms, and a spatial resolution of 0.9 mm^3. For each subject, localization of the LGN was performed in a separate session with identical acquisition parameters.

MRI data were processed using Brain Voyager QX 2.6.1 (Brain Innovations, Maastricht, The Netherlands). Functional resolution was preserved at the original acquisition resolution (3.0 mm^3) throughout the entire analysis pipeline. Anatomical data of each observer were used for cortex reconstruction, inflation, and flattening. The initial volume of each functional run was discarded in order to eliminate effects of startup transients in the data. Functional data were pre-processed using slice-time correction, three-dimensional motion correction, linear trend removal, and highpass filtering (three cycles per run cut-off). The functional images were then aligned to each participant's anatomical data and transformed into Talairach space (Talairach & Tournoux, 1988). For each observer, functional data between different sessions

were co-aligned. All volumes of each observer were aligned to the first functional volume of the first run of the session.

For the ROI-based percent signal-change-analyses (described below), responses were time-shifted to account for hemodynamic lag (1 TR, 3 s). We chose to perform a percent signal change analysis rather than fitting the data to a regression model as it is unclear as to how adaptation might distort the underlying HRF model; moreover, we gain through the PSC analysis a more transparent and intuitive unit-interpretation metric.

Regions of interest

For each participant, we identified two regions of interest corresponding to the lateral geniculate nucleus (LGN) and the superior colliculus (SC). The LGN was identified for each subject both in accordance with well known anatomical landmarks (Kastner et al., 2004) and via an independent functional localizer (Fig. 2A) (Mullen et al., 2008; Hess et al., 2009). Our localizer contrasted a high-contrast checkerboard stimulus with both chromatic and achromatic contrast flickering (16 Hz) with both AC and DC modulation with a blank screen. LGN clusters were then restricted to ensure exclusion of overlapping voxels with the nearby pulvinar, including in particular, the visually responsive ventral pulvinar (Kastner et al., 2004; Cotton & Smith, 2007; Smith et al., 2009; Schneider, 2011) which has strong functional connections to the early and extrastriate cortex (Arcaro et al., 2015), the ventral-lateral nucleus, and the ventral-posterior-lateral nucleus, as identified from probabilistic and Talairach atlases (Oxford thalamic connectivity atlas, Behrens et al., 2003a, b) and transformed into Talairach space. The final LGN ROIs had average Talairach locations and volumes of [−22 (±3.3), −24 (±2.3), −1 (±2.3); 294 mm^3], and [19

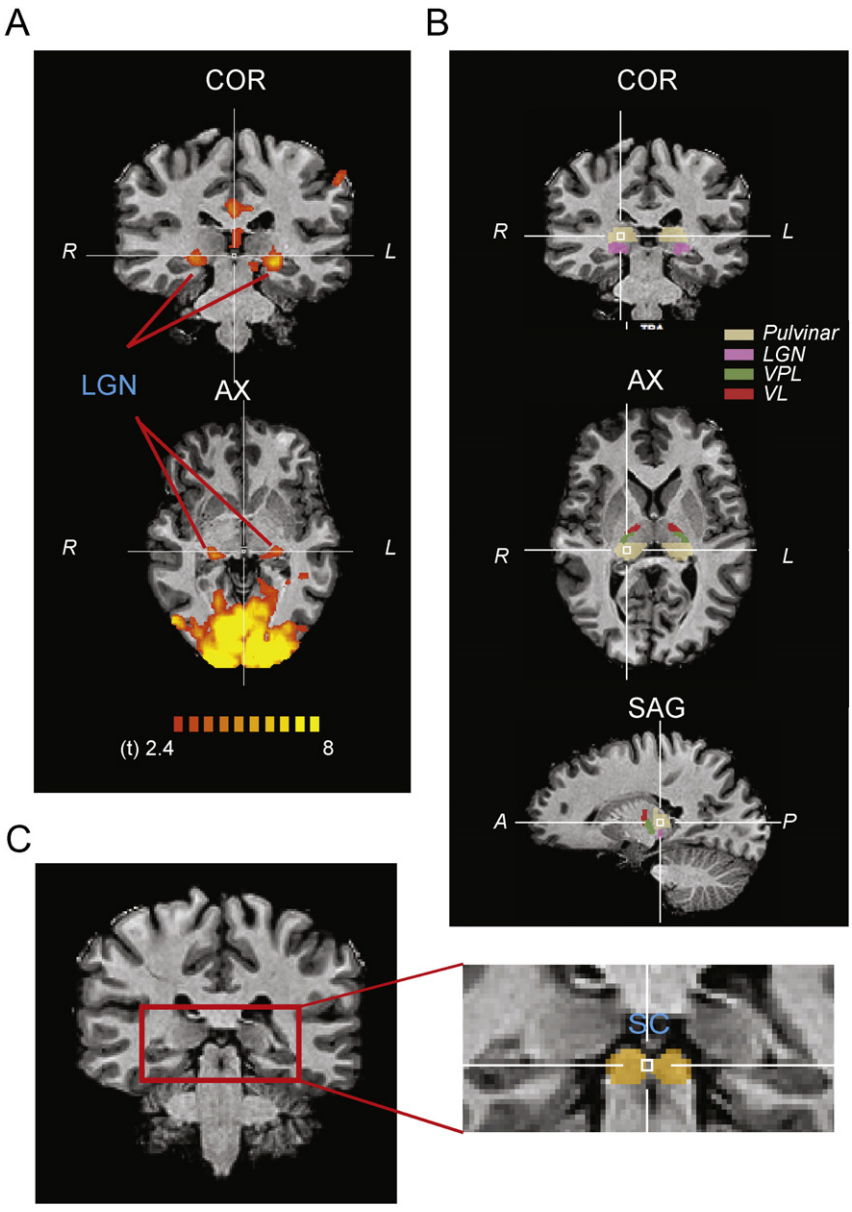

Fig. 2. Localization of subcortical structures. (A) The LGN was identified for each subject both in accordance with well known anatomical landmarks (Kastner et al., 2004) and via an independent functional localizer that contrasted a high-contrast checkerboard stimulus with both chromatic and achromatic contrast flickering (16 Hz) with both AC and DC modulation with a black screen (Mullen et al., 2007). Note the activity map is overlaid on to the high resolution 1 mm^3 anatomy, but functional data were retained in 3 mm^3 resolution throughout the analysis pipeline. (B) LGN ROIs were subsequently restricted to ensure exclusion of the pulvinar and other nearby thalamic structures. The crosshair is on the pulvinar. The coronal view shows the ventral location of the LGN relative to the pulvinar. Below, the corresponding axial and sagittal view shows locations of the other nuclei relative to the pulvinar. The LGN falls ventrally and is not visible from this particular slice/view. (C) The superior colliculus (SC) was defined for each subject, based on anatomical inspection, guided by an anatomical and radiological brain atlas (Duvernoy, 1999).

(±3.8), −24 (±2.8), −1 (±2.1); 270 mm^3] for the left and right LGN, respectively. These coordinates and volumes are consistent with those identified previously (Kastner et al., 2004; Mullen et al., 2008). The superior colliculus (SC) was defined anatomically for each subject based on inspection of their anatomical MRI image, guided by an anatomical and radiological brain atlas (Duvernoy, 1999) and coordinates previously reported by Schneider and Kastner (2005) (see also, Petit & Beauchamp, 2003) (Fig. 2B). Care was taken to ensure that each SC ROI did not extend into the adjacent midbrain areas. The SC ROIs identified in this manner had mean Talairach coordinates of [−5 (±0.8), −28 (±1.0), −3 (±0.5)] for the left SC and [5 (±0.5), −28 (±1.0), 3 (±0.5)] for the right SC. These locations are similar to those previously reported (Schneider & Kastner, 2005; Petit and Beauchamp, 2003).

For each region of interest, we normalized the raw data by selecting the mean signal during all fixation intervals as baseline and computing for each voxel (at each time point), a percent signal change relative to the mean of fixation baseline. For each run (RG-adapt or ACH-adapt), we then computed mean percent signal change separately for each test (RG, ACH) independently following adaptation and no adaptation intervals. For each ROI and for each test stimulus, the effect of adaptation was quantified by comparing (differencing) the responses following adaptation versus no adaptation during the test period (excluding the first test TR), independently for each adaptor type (RG, ACH), yielding a difference score (termed *signal loss*).

Results

Sensitivity of human LGN and SC to chromatic and achromatic contrast

We first tested the response of our ROIs to the red–green and achromatic stimuli. The mean percent signal change responses to both RG and ACH test stimuli following the no (blank) adapt periods are presented separately for the two regions in Fig. 3, collapsed across both types of adapting runs. An examination of this figure reveals that both ROIs have a measurable response to the two types of stimuli in the absence of adaptation. Although the responses to the RG stimulus are larger than those to the ACH stimulus, the difference does not reach statistical significance, as revealed by a 2 (Test — RG/ACH) × 2 (Adaptor Type — RG/ACH) × 2 (ROI — LGN/SC) repeated measures ANOVA. The analysis showed a marginal effect of Test type [$F(1,12) = 3.7$, $p = .08$], but no significant main effect of Adaptor [$F(1,12) = .08$, $p = .79$], and no significant main effect of ROI [$F(1,12) = .11$, $p = .74$]. The test responses measured in the no-adapt condition were the same whether obtained as part of the RG or ACH adaptation runs (as expected) and so we pooled the data from the two adapting runs in this figure. Note however that in computing the adaptation effect (signal loss, below), the specificity of the blank adapt test data was maintained (i.e., using unpooled data). The unpooled time series response of the test stimuli without (dashed) and with (solid) adaptation is also provided in Fig. S1 (shaded regions).

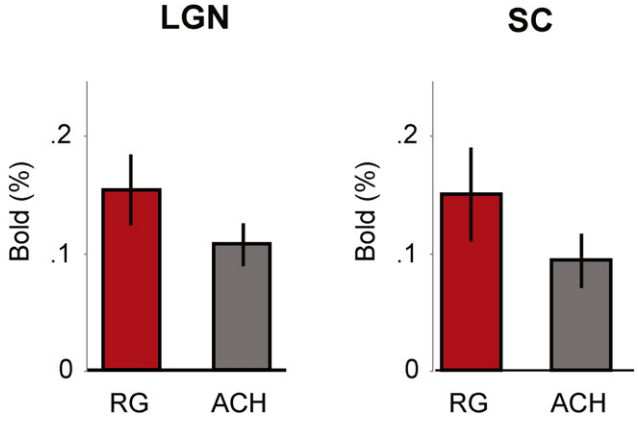

Fig. 3. Responses of the LGN and SC to the red–green (red fill) and achromatic (gray fill) stimuli without adaptation (i.e., tests following blank adapt). The raw responses for the tests are presented separately for each ROI (LGN, SC), pooled across both red–green and achromatic adapting runs. Error bars represent ±1 standard error.

Adaptation

Next, we asked whether the LGN and SC show effects of contrast adaptation, defined as a weaker test signal following the viewing of the adaptor versus a blank interval, and if so, whether adaptation is selective for the type of contrast presented (chromatic or achromatic). In Fig. 4, we further separate the mean time series data for the two ROIs (A, LGN; B, SC), reorganizing the data by test stimulus (test RG or test ACH) for better clarity. In each panel, we present the data during the adaptation period (adapt RG or ACH, no adapt), the test period (test ACH or RG following adapt versus no adapt), and the fixation period. The response to the test stimuli following no (blank) adapt rises and is followed by a shallow decline towards the end of the test period. The response to the test *after* adaptation, however, is very different and contingent upon the particular type of adaptor that preceded this period and the particular test considered. For the RG test, the signal is markedly depressed following the RG adaptor and remains low, and also significantly declines following the ACH adaptor (albeit more slowly). For the ACH test, the test signal shows a weaker decline, regardless of adaptor type. For each test stimulus, we quantified the adaptation effect in terms of a signal loss, computed by differencing the test response after adaptation from that with no adaptation for each participant (i.e., the difference between the dashed and the solid lines during the shaded period in Fig. 4), discarding the first test period TR. The mean responses during this period following adaptation are presented in Fig. 5A & C, and are compared to the mean responses to the stimuli without adaptation (empty bars). For each test stimulus, the mean adaptation effect in terms of signal loss is also presented (Fig. 5B & D).

As evident from this figure the responses of the LGN and SC to the RG stimulus are markedly reduced following adaptation to both the RG stimulus and the ACH stimulus Fig. 5A & B). By contrast, for both ROIs, responses to the ACH stimulus show weak or no adaptation (Fig. 5C & D). Inspection of Fig. 4 reveals small adaptation effects for the ACH conditions that is reflected in small losses of Fig. 5D. However, these effects are weak and do not reach statistical significance. A four-way repeated-measures ANOVA [2 (Test — RG/ACH) × 2 (Adaptation — Blank/Adapt) × 2 (Adaptor — RG/ACH) × 2 (ROI — LGN/SC)] indicated a significant main effect of Adaptation [$F(1,12) = 47.9$, $p < .001$], and a significant Test by Adaptation interaction [$F(1,12) = 12.5$, $p = .004$]. The interaction was followed up with an independent three-way ANOVA for each test. The analysis for the RG test indicated a significant main effect of Adaptation [$F(1,12) = 42.0$, $p < .001$]. By contrast, the analysis for the ACH test indicated no main effect of Adaptation [$F(1,12) = 2.4$, $p = .144$]. Considered together, the analyses indicate significant adaptation for the RG test response (for both adaptors) but not for the ACH test response. For the RG test, while there is a trend towards greater adaptation by the RG than the ACH adaptor, the interaction does not reach statistical significance.

As noted earlier, the base (no-adapt) responses were marginally, although not significantly larger for the RG test than for the ACH test. In order to remove any possible effect of this small difference, in Fig. S2, we recompute the adaptation effect in terms of a normalized signal loss, computed by normalizing the difference scores (no adapt − adapt) to the sum of the adapt and no-adapt responses (no-adapt + adapt) response. A repeated-measures ANOVA on these normalized losses indicated a significant main effect of test only [$F(1,12) = 7.2$, $p = .02$], reflecting the fact that the normalized signal loss is greater for the RG test than for the ACH test. Additional Bonferroni-corrected comparisons indicate that the normalized loss is significantly greater than zero for the RG test ($p < .05$ for all), but not

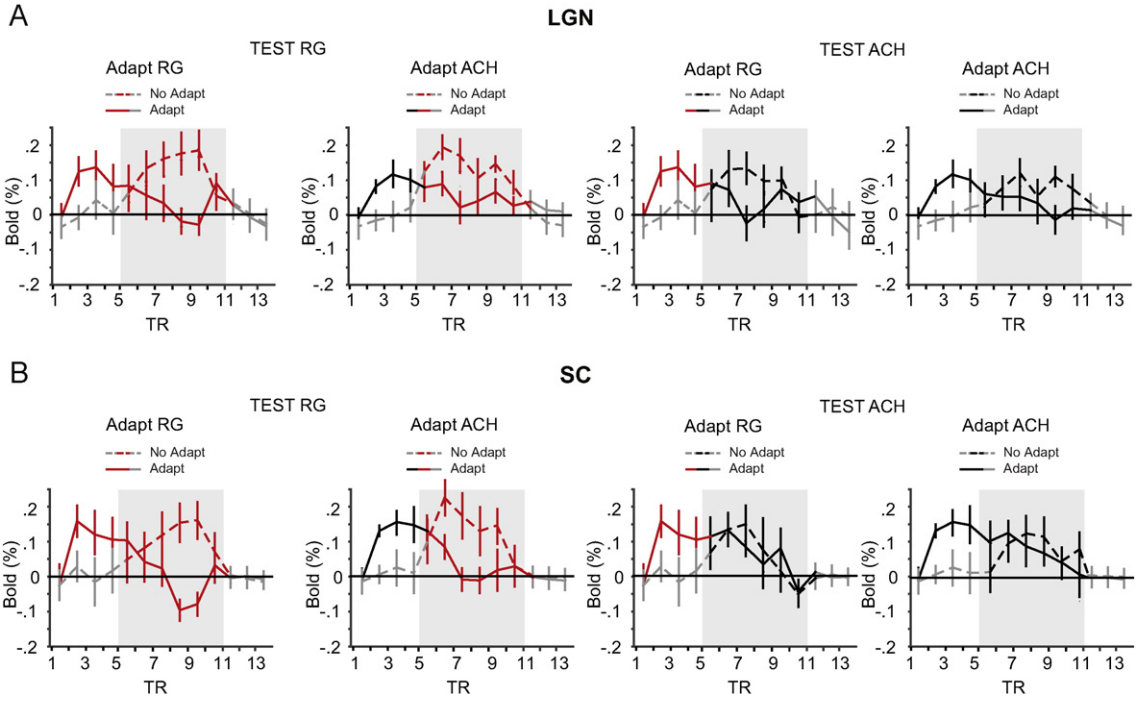

Fig. 4. Mean time series data for the LGN (A) and SC (B). Data are presented for the adaptation and no adaptation conditions (first 4 TRs), the test conditions (TRs 5–10, shaded), and the fixation condition (TRs 11–13) separately for the RG (left panels) and ACH tests (right panels) following adaptation (solid lines) and no adaptation (dashed lines). Error bars represent ±1 standard error. The response to a particular test was computed as the mean response for the shaded period, discarding the first TR. The adaptation effect was quantified as a difference in test response following no adapt and adaptation conditions (i.e., difference between the dashed and solid test lines). As the signal measured for each TR is a binned, mean signal acquired during the 3 second period, data points are placed midway between the tick-marks indicating the end of each TR.

the ACH test ($p > .11$ for all). Interestingly, further inspection of the normalized data reveals that the RG adaptor results in a greater signal loss for the ACH test than the ACH adaptor (although neither is significantly different from zero). As these results are consistent with the original analyses on the raw differences, we retain the original representations.

As our full data set included measurements from two scanners, we additionally compared adaptation effects between the two machines (Supplementary Fig. S3). The adaptation trends are very similar for both the 4 Tesla ($n = 4$) and 3 Tesla ($n = 9$) scanners. For both scanners, the response for the RG test (for both ROIs) shows strong adaptation to the RG stimulus and weaker but substantial cross-adaptation to the ACH stimulus. By contrast, the response to the ACH stimulus shows weak or no adaptation by either stimulus. This is supported by a mixed ANOVA for Scanner (4 T/3 T) × Test (RG/ACH) × Adaptation (Adapt/No Adapt) × Adaptor (RG/ACH) × ROI (LGN/SC) that indicated a significant Test by Adaptation interaction only [$F(1,11) = 16.6$, $p = .002$]. Congruent with the overall, group-level findings, the response for the RG test (for both ROIs) shows strong adaptation to the RG stimulus and substantial cross-adaptation to the ACH stimulus. By contrast, the response to the ACH stimulus shows weak or no adaptation by either stimulus. This indicates that our adaptation effects are robust and replicable.

Next, due to our large stimulus size and concerns over potential changes in isoluminance (and therefore adaptation effects) across the visual field, we examined the consistency of the adaptation effects within the ROI by partitioning the LGN of each participant into medial (eccentric) and lateral (foveal) segments. While we are limited by our relatively large resolution in relation to the size and shape of the LGN, this division allowed us to retrieve activity from distinct voxels in the two segments. We recomputed the effects with this division and present them in Fig. S4. The adaptation effects are very comparable between the more medial (eccentric) and lateral (foveal) segments.

Finally, we considered the consistency of our adaptation effects at the individual-subject level by plotting for each subject, their adaptation effect (quantified as signal loss) for each of the four main conditions (2 adaptors × 2 tests) (Supplementary Fig. S5). In each panel, the adaptation effect can be compared for the two tests by examining the direction of the subject along the X- (test RG) and Y- (test ACH) axes. For most subjects, the adaptation effect for the RG test is robust, falling in the positive x-direction. By contrast, the individual adaptation effects for the ACH test are weak and inconsistent.

Adaptation at the end of the test period

As our test period is relatively long we asked whether adaptation effects have disappeared by the end of the test period by computing the adaptation effect (signal loss) at the final test TR, 18 s after the onset of the test period (Fig. 6). As reflected in the figure, adaptation effects have largely disappeared by the end of the test interval (c.f., Fig. 5). This is confirmed by a four-way repeated-measures ANOVA [2 (Test — RG/ACH) × 2 (Adaptation — Blank/Adapt) × 2 (Adaptor — RG/ACH) × 2 (ROI)] that indicated no main effect of Adaptation [$F(1,12) = .38$, $p = .55$] and no interactions.

Behavioral contrast discrimination

In order to control for attention and stimulus difficulty, observers performed a contrast discrimination task throughout each scan run. We present the mean discrimination accuracies (proportion correct) for the two adapting runs independently for the two tests in Supplementary Fig. S6. Accuracies for the two types of adaptors and the two tests are very similar (84–88%). A three-way repeated measures ANOVA comparing accuracies for adaptor type (2) × adaptation (2) × test (2), showed no significant main effects of Adaptor type [$F(1,12) = .46$, $p = .51$], Adaptation [$F(1,12) = .28$, $p = .61$], or Test, [$F(1,12) = 3.1$, $p = .10$], and no interactions. These data suggest that the differences in the fMRI adaptation effects cannot be accounted for by simple differences in stimulus demands.

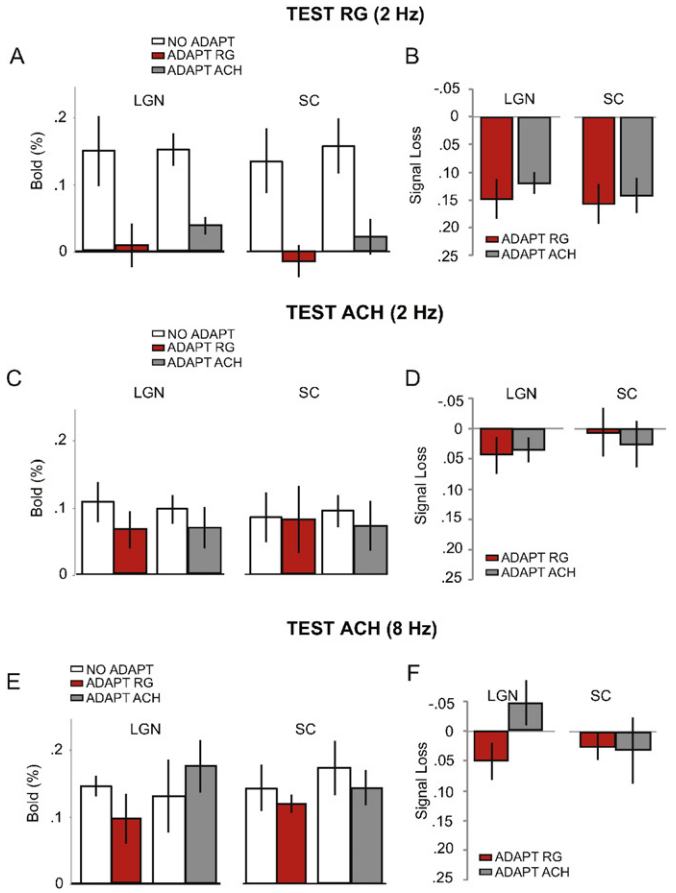

Fig. 5. Raw responses of the LGN and SC to red–green (A) and achromatic (C) stimuli following chromatic (red fill) and achromatic (gray fill) adaptation obtained under 2 Hz. For comparison, we again present the test responses without adaptation but unpooled (empty bars). The adaptation effect is quantified as a signal loss, computed as the difference in response between the adapt and no-adapt conditions. These signal losses are presented for the red–green (B) and achromatic tests (D). Raw response (E) and signal loss (F) data from a control experiment testing achromatic responses and adaptation at 8 Hz (see 0Adaptation of the achromatic stimulus at 8 Hz section). Error bars represent ±1 standard error.

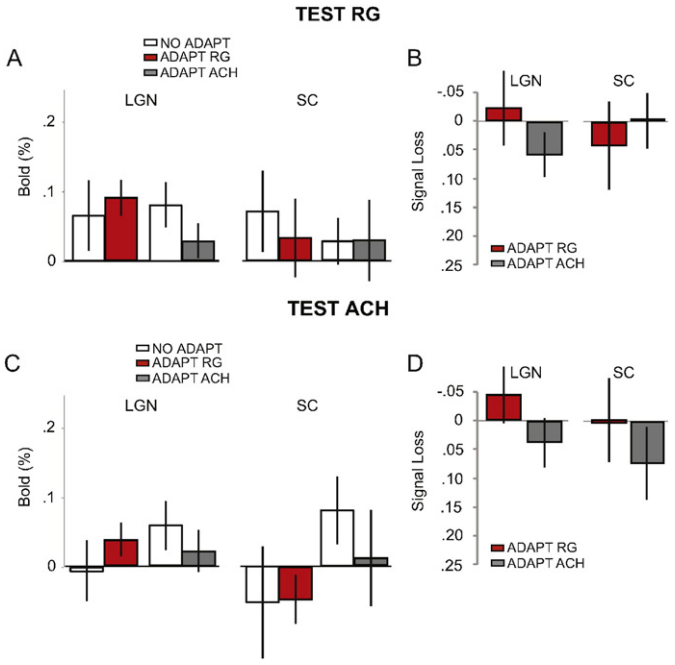

Fig. 6. Responses and the adaptation effect (signal loss) for the final TR of the test period. For each ROI, the raw responses of the LGN and SC to red–green (A) and achromatic (B) tests following chromatic (red fill) and achromatic (gray fill) adaptation, and without adaptation (empty bars) are presented. The signal loss at this final TR is also presented for the RG (C) and ACH (D) tests, independently for the RG and ACH adaptors. Error bars represent ±1 standard error.

Adaptation of the achromatic stimulus at 8 Hz

The lack of an adaptation effect for the achromatic stimulus in the main experiment may reflect a genuine lack of ACH adaptation, lack of statistical power, or reflect that our choice of stimulus parameters is generating a relatively weak base achromatic response in these regions. As noted above, the base no-adapt response to the ACH stimulus was lower, although not statistically different from the base response to the RG stimulus. In order to rule out potential floor-effects for the ACH test data, we completed a control experiment on four of the original participants. In this additional experiment, the temporal frequency of the stimuli was increased to 8 Hz as previous work indicated that this higher temporal frequency may provide a stronger ACH response in the LGN (Mullen et al., 2010). As before, participants completed two sessions on separate days, one for each adaptor type, but adaptation effects were probed for the ACH stimulus only, as only this, and not the chromatic response, will be boosted at higher temporal frequencies (Mullen et al. 2010).

The time series results of the 8 Hz experiment are presented in Fig. S7. The base, no-adapt signal for the ACH test at 8 Hz is higher than that obtained previously for 2 Hz, and is comparable to that for the RG test under 2 Hz (c.f., Fig. 4). As before for ACH stimuli, the signal shows a weak decline following adaptation, regardless of adaptor type.

In Fig. S8A, the mean test responses following adaptation (solid bars) are compared to those without adaptation (empty bars). For each test stimulus, the mean adaptation effect is also presented in terms of raw signal losses in Fig. S8B (c.f., Fig. 5D), and normalized losses in Fig. S8C (c.f., Fig. S2B). We also reproduce these graphs alongside the main data in Fig. 5E, F. Inspection of these data again reveal that the no-adapt signal for the ACH test under 8 Hz is now more comparable to that for the RG test under 2 Hz (c.f., Fig. 5A), suggesting that the higher temporal frequency resulted in a stimulus that is a better driver for the M-cell-type (achromatic) responses. Despite this elevated baseline response, however, it is also clear that there remains no signal loss (adaptation effect) in either the LGN or SC following either the ACH or RG adaptor, suggesting that floor effects (or poor driver responses) are unlikely to account for the lack of adaptation for the ACH stimulus in the main experiment.

Taken together, the results indicate that the human subcortical structures considered here are sensitive to both chromatic and achromatic contrast and show a capacity for adaptation. Notably, adaptation to the red–green stimulus is robust for both types of adaptors. The presence of the strong cross adaptation indicates that the neural response to the RG test stimuli is unselective. This would be consistent with a P cell system that is responsive in some way to achromatic as well as chromatic information (for example, as in the "double duty" hypothesis, Lennie & D'Zmura, 1988; Lennie et al., 1991).

Discussion

We tested the adaptation of human subcortical structures LGN and SC to red–green and achromatic contrast using an fMRI adaptation protocol. We show that the LGN exhibits robust activity in response to chromatic and achromatic contrast without the presence of the adaptor, in line with previous work (Mullen et al., 2008; Hess et al., 2010; Mullen et al., 2010; Zhang et al., 2015). We show for the first time that the human LGN does in fact have a significant capacity for adaptation. Moreover, the adaptation measured is restricted to the red–green test

response and is unselective to the type of adaptor, revealing an influence of achromatic contrast on the chromatic RG response. Using the same adaptation method, we have previously shown widespread adaptation in the cortex to both achromatic and chromatic (RG) stimuli, with robust unselective adaptation to both types of contrast in the early cortical areas (V1, V2) (Mullen et al., 2015). Given the extensive reciprocal connections between the two structures (e.g., Butt et al., 2015; Genç et al. 2015; Sherman, 2016), we might have expected to observe pronounced adaptation for the ACH stimulus in the LGN as we did in V1. Instead, we find that under identical testing parameters, adaptation of ACH contrast is weak or absent in the LGN. The data suggest that adaptation of early cortex cannot be fully accounted for by bidirectional thalamocortical projections, and perhaps point to a need to consider an additional role for intracortical connections (Burkhalter & Bernardo, 1989).

Nonetheless, while in the early cortex, we showed robust but unselective adaptation (for both RG and ACH stimuli), color selective adaptation emerged in the extrastriate ventral areas, especially VO, and selective processing of ACH contrast emerged in the dorsal areas (Mullen et al., 2015). Our results for the LGN thus fit the broad pattern of unselective processing as characteristic of the early visual system.

We also considered chromatic response adaptation in the human SC — a region belonging to the saccadic system that has long been assumed to be color-blind (e.g., Marrocco & Li, 1977; Schiller & Malpeli, 1977; Leh et al., 2009) but recently shown to be responsive to chromatic signals in both non-human primates (Hall & Colby, 2014; Herman & Krauzlis, 2014) and humans (Zhang et al., 2015). We show that the human SC not only responds to red–green color contrast but, like the LGN, also shows significant but unselective adaptation — effects possibly carried by broadly tuned neurons in intermediate or superficial layers with transcortical access to traditional color regions (see below).

As we did not measure behavioral adaptation effects, we cannot speculate as to the correspondence between our measured fMRI adaptation effects and behavioral contrast adaptation. We note however that a previous study using test stimuli (gratings) defined with an identical or similar contrast (4% for RG and 7% for ACH) demonstrated significant behavioral adaptation using a color-matching task. Moreover, behavioral adaptation patterns matched well to measured fMRI adaptation effects in the cortex (Engel & Furmanski, 2001). Interestingly, the authors reported less selective behavioral adaptation effects using the 2 Hz stimulus (identical to that used in the present study), as compared to the 8 Hz stimulus. Here, we observed significant fMRI adaptation that also appears rather unselective (i.e., robust cross-adaptation for the RG test) in both ROIs.

Lateral geniculate nucleus

While much literature assumes that red–green and achromatic behavioral responses are unique to the P- and M-pathways, respectively (e.g., Lee et al., 1990), others have argued for a “double duty” role for P cells as driver neurons responsive to both chromatic and achromatic contrast (Lennie & D'Zmura, 1988; Lennie et al., 1991; Merigan et al., 1991). Here, we found significant adaptation of the P-cell-activating, red–green stimulus, with adaptation generated unselectively by both types of adaptors. The robust cross-adaptation observed here suggests that the P-pathway does in fact have access to achromatic as well as chromatic information, potentially supporting a common role of P cells for both achromatic and red–green contrast responses. It remains unspecified, however, exactly how this unselective response may be established. The cross adaptation may reflect the fact that responses of P cells can be driven by both chromatic and achromatic contrast, as has been widely reported in primates (Derrington et al., 1984; Lee et al., 1990). Alternatively, an effect of achromatic or chromatic contrast may arrive via descending modulatory inputs from the cortex and other subcortical brain structures (including the SC). While feed-forward connections from the LGN provide the striate cortex with visual information from the retina, axons from cortico-thalamic neurons also project directly back to the LGN. In the macaque, there is even evidence for some degree of segregation of cortico-thalamic projections with the lower layer 6 projecting to the magnocellular and upper layer 6 projecting to parvocellular compartments of the LGN (Lund & Boothe, 1975; Wiser & Callaway, 1996). The influence that layer 6 in the striate cortex has on thalamic neurons is still controversial, although orientation and direction tuning, and gain control in the thalamus all appear to be influenced by the cortex (e.g., Sillito et al., 1994, Ling et al., 2015; O'Connor et al., 2002). Layer 6 corticothalamic feedback seems to modulate not only thalamo-cortical input, but also retino-geniculate input (for a recent review of the modulatory role of cortical input on the thalamus, see also Sherman, 2016). It is reasonable to suggest that color signals in the LGN may also be modulated by projections from both the achromatic and chromatic cortical networks, contributing to the unselective adaptation effects observed here. Furthermore, BOLD responses of the LGN are likely to reflect descending cortical modulation more than the ascending driver neuron responses because these synapses are vastly more numerous (Sherman & Guillery, 2002, 2011; Sherman, 2016).

Our data appear at odds with those reported from single unit recordings in the macaque (Solomon et al., 2004). Solomon et al. (2004) who, using only achromatic stimuli, showed that neurons in the magnocellular LGN (M cells) have strong contrast adaptation compared to little adaptation in parvocellular LGN (P cells). The source of this adaptation was shown to be retinal in origin. Since the LGN red–green responses are mediated by P cells, our results indicate robust adaptation in the LGN P cell pathway. Also, we found very little, if any, contrast adaptation to achromatic stimuli, yet in single cell recording adaptation was found only in M cells. We think this difference may be explained by at least two different factors. First, the two techniques reveal different aspects of LGN function. As already discussed, the LGN BOLD response is likely to be more influenced by descending cortical connections than the ascending driver neuron responses. In fact there are a number of fMRI studies in which the LGN BOLD responses appear to reflect the properties of V1 better than the properties of the driver neurons (e.g. Ling, Pratte & Tong, 2015 for orientation; Mullen et al., 2010 for temporal frequency; O'Connor et al., 2002 for attention). Because the M cell population is very sparse, any adaptation effects may be undetectable in the BOLD response, especially as our localizer protocol and resolution did not permit the M and P layers to be segregated (however, see Denison et al., 2014; Zhang et al., 2015). Nevertheless, it is very interesting that fMRI reveals a strong adaptation of the P-cell mediated, chromatic response by both achromatic and chromatic contrast, when single cell recordings show no P-cell adaptation.

Second, there are differences between the two studies in the choice of stimulus parameters. We considered whether the lack of achromatic adaptation in the main experiment may, at least in part, be due to our choice of a low temporal frequency stimulus (2 Hz), especially as gratings modulating at low temporal frequencies compared to higher ones have been shown to be weak adaptors of M cells in both the macaque (Solomon et al., 2004, Fig 4a) and cat (e.g., Maffei et al., 1973; Movshon & Lennie, 1979; Ohzawa et al., 1985). We found that the human LGN response to the achromatic stimulus increased marginally from 2 Hz to 8 Hz and we ran an additional control experiment to further test for adaptation of the achromatic response using a higher (8 Hz) temporal frequency. Despite attaining a higher baseline and a no-adapt signal that is comparable to that observed for the RG test stimulus at 2 Hz, the achromatic stimulus again displayed little adaptation, suggesting that the lack of adaptation observed at 2 Hz also extends to 8 Hz even with the increased base-line response.

Superior colliculus

Very little is known about the visual response properties of the human SC. A small body of literature has yielded insight into the anatomical organization of the human SC including its cellular morphology, laminar pattern (Laemle, 1981; Hilbig et al., 1999), columnar organization

(Graybiel, 1979), and connections (Tardif & Clarke, 2002). Functional imaging studies in human SC to date have shown activity relating to the deeper layer-type functions such as eye movements (Petit & Beauchamp, 2003; Schmitz et al. 2004), and tasks relating to spatial navigation and visual search (Grön et al. 2000; Gitelman et al. 2002). Using fMRI, visual field maps have been identified in the SC (DuBois & Cohen, 2000; Schneider & Kastner, 2005; Wall et al., 2009). Topographic maps can also be revealed by directed (covert) visual attention, in addition to visual stimulation (Katyal et al., 2010). Finally, the SC has been implicated in blindsight — responding when an achromatic (but not an S-cone isolating) stimulus is presented in the blind visual field (Leh et al., 2009). The role of RG stimuli in blind sight has not yet been established (Leh et al. 2006).

Color plays an important role in image segmentation and aids in visual search (D'Zmura et al., 1997), yet the system that controls saccadic eye movements and directed attention in primates has long been thought to be color-blind (Schiller et al., 1979). This is in contrast to behavioral evidence that human observers are well able to make saccades or a rapid pointing movement to isoluminant, chromatic stimuli (White et al., 2006). In fact, White et al. (2006) found no difference in the accuracy of saccades or rapid pointing movements to targets defined exclusively by luminance or color. More recent neurophysiological data from the macaque have indicated that neurons in the intermediate (but not superficial) layers of the SC do in fact have access to color information — responding with the same magnitude to isoluminant (red–green) color stimulus as to a luminance stimulus (White et al., 2009). Neurons of the primate SC have been further shown to respond robustly to the S-cone isolating (blue–yellow) stimulus (Hall & Colby, 2014; Herman & Krauzlis, 2014).

In line with primate neurophysiological evidence, and human psychophysics and fMRI (Zhang et al., 2015), we find robust responses to red–green chromatic contrast in the human SC. Significantly, we show that, like the LGN, the SC shows significant but unselective adaptation (i.e., the chromatic response is similarly affected by both our RG and ACH adaptors). How might the SC gain access to information about color? The saccadic system receives a large number of direct and indirect projections from the visual cortex (e.g., Sommer & Wurtz, 2004), which are likely to provide access to color signals. The superficial layers of the SC receive projections from early visual areas V1, V2, as well as dorsal V3, and MT (Fries, 1984; Lock et al., 2003). Regions that project to the intermediate SC are also extensive, including the frontal cortex and extrastriate visual areas typically associated with color such as V4 (Fries, 1984; Lock et al., 2003). As we do not have the resolution to distinguish between contributions of the different layers of the SC using our methods, our adaptation effects may originate from layers at either depth with transcortical access.

A possible account for the similar adaptation effects observed in both the LGN and SC is that adaptation in both regions is inherited from the retina. While the origin of fMRI adaptation at the level of the cortex can perhaps be better evaluated through measures of orientation selectivity, most neurons in the primate LGN have receptive fields that are circularly symmetric with little orientation tuning. Thus, it would not be straightforward to tease apart retinal versus thalamic origins of the adaptation effects observed here. Although orientation signals have been demonstrated in the human LGN, they are likely enhanced by, if not entirely delivered by cortical feedback (Ling et al., 2015).

As fMRI (BOLD) signals in the LGN and SC have been shown to be weak in response to the S-cone (blue–yellow) contrast (Mullen et al., 2008, Leh et al., 2009; D'Souza et al., 2011), we presumed that any adaptation effect would be too weak to measure and did not pursue measurements of the S-cone stimulus here in either structure. It is still interesting to consider the wider implications of recent neurophysiological data showing robust S-cone input to the SC (Hall & Colby, 2014; Herman & Krauzlis, 2014), contrary to earlier findings (Tailby et al., 2012). These data call into question the use of the S-cone stimuli for examining the function of the SC in phenomena such as blindsight (Leh et al., 2006, 2009). Indeed, our data suggest that the role of the SC in blindsight is likely not purely achromatic, as we find strong input from the red–green (P) system in healthy-sighted individuals, which has not yet been systematically tested.

Summary

We show that the human LGN not only exhibits sensitivity to chromatic as well as achromatic contrast but the chromatic response has significant capacity for adaptation. These findings are in contrast to neurophysiological data from non-human primates that have shown weak, or no contrast adaptation in the P pathway. The strong cross adaptation of the RG response suggests that the P pathway has access to achromatic information, supporting a dual role for this system. We further show that subcortical adaptation is not isolated to the LGN and is also present in the SC of the retinotectal pathway — a region that has, until relatively recently, been thought to be color-blind. We show in fact that the human SC, like the LGN, is not only capable of signaling the presence of chromatic (and achromatic) stimuli, but also shows significant chromatic adaptation.

Acknowledgments

This work was supported by the Canadian Institutes of Health Research (MOP-10819 to K.T.M. and MOP-53346 to R.F.H.). We thank Irem Onay for her assistance in data collection and Ben Thompson for his contribution to the data analysis at an early stage of the work.

Appendix A. Supplementary data

Supplementary data to this article can be found online at http://dx.doi.org/10.1016/j.neuroimage.2016.04.067.

References

Arcaro, M.J., Pinsk, M.A., Kastner, S., 2015. The anatomical and functional organization of the human visual pulvinar. J. Neurosci. 35 (27), 9848–9871.
Baccus, S.A., Meister, M., 2002. Fast and slow contrast adaptation in retinal circuitry. Neuron 36, 909–919.
Behrens, T.E.J., et al., 2003a. Non-invasive mapping of connections between human thalamus and cortex using diffusion imaging. Nat. Neurosci. 6 (7), 750–757.
Behrens, T.E.J., et al., 2003b. Characterisation and propagation of uncertainty in diffusion weighted MR imaging. Magn. Reson. Med. 50, 1077–1088.
Blakemore, C., Campbell, F.W., 1969. On the existence of neurones in the human visual system selectively sensitive to the orientation and size of retinal images. J. Physiol. 203, 237–260.
Bradley, A., Zhang, L., Thibos, L.N., 1992. Failures of isoluminance caused by ocular chromatic aberration. Appl. Opt. 31, 3657–3667.
Brainard, D.H., 1997. The psychophysics toolbox. Spat. Vis. 10, 433–436.
Brown, S.P., Masland, R.H., 2001. Spatial scale and cellular substrate of contrast adaptation by retinal ganglion cells. Nat. Neurosci. 4, 44–51.
Burkhalter, A., Bernardo, K.L., 1989. Organization of corticocortical connections in human visual cortex. Proc. Natl. Acad. Sci. 86, 1071–1075.
Butt, O.H., Benson, N.C., Datta, R., Aguirre, G.K., 2015. Hierarchical and homotopic correlations of spontaneous neural activity within the visual cortex of the sighted and blind. Front. Hum. Neurosci. 9 (25), 1–11.
Camp, A.J., Tailby, C., Solomon, S.G., 2009. Adaptable mechanisms that regulate the contrast response of neurons in the primate lateral geniculate nucleus. J. Neurosci. 29, 5009–5021.
Carandini, M., Movshon, J.A., Ferster, D., 1998. Pattern adaptation and cross-orientation interactions in the primary visual cortex. Neuropharmacology 37, 501–511.
Chander, D., Chichilnisky, E.J., 2001. Adaptation to temporal contrast in primate and salamander retina. J. Neurosci. 21, 9904–9916.
Cottaris, N.P., 2003. Artifacts in spatiochromatic stimuli due to variations in preretinal absorption and axial chromatic aberration: implications for color physiology. J. Opt. Soc. Am. A Opt. Image Sci. Vis. 20, 1694–1713.
Cotton, P.L., Smith, A.T., 2007. Contralateral visual hemifield representations in the human pulvinar nucleus. J. Neurophysiol. 98, 1600–1609.
Cowey, A., Stoerig, P., Hodinott-Hill, I., 2003. Chromatic priming in hemianopic visual fields. Exp. Brain Res. 152, 95–105.
Cynader, M., Berman, N., 1972. Receptive-field organization of monkey superior colliculus. J. Neurophysiol. 35, 187–201.
D'Souza, D.V., Auer, T., Strasburger, H., Frahm, J., Lee, B.B., 2011. Temporal frequency and chromatic processing in humans: an fMRI study of the cortical visual areas. J. Vis. 11 (8), 8.
D'Zmura, M., Lennie, P., Tianoa, C., 1997. Color search and visual field segregation. Percept. Psychophys. 59, 381–388.
Denison, R.N., Vu, A.T., Yacoub, E., Feinberg, D.A., Silver, M.A., 2014. Functional mapping of the magnocellular and parvocellular subdivisions of human LGN. NeuroImage 102, 358–369.

Derrington, A.M., Krauskopf, J., Lennie, P., 1984. Chromatic mechanisms in lateral geniculate nucleus of macaque. J. Physiol. 357, 241–265.
Derrington, A.M., Lennie, P., 1984. Spatial and temporal contrast sensitivities of neurones in lateral geniculate nucleus of macaque. J. Physiol. 357, 219–240.
DuBois, R.M., Cohen, M.S., 2000. Spatiotopic organization in human superior colliculus observed with fMRI. NeuroImage 12, 63–70.
Duvernoy, H.M., 1999. The Human Brain. Springer-Verlag, New York.
Engel, S.A., 2005. Adaptation of oriented and unoriented color-selective neurons in human visual areas. Neuron 45, 613–623.
Engel, S.A., Furmanski, C.S., 2001. Selective adaptation to color contrast in human primary visual cortex. J. Neurosci. 21, 3949–3954.
Fang, F., Murray, S.O., Kersten, D., He, S., 2005. Orientation-tuned FMRI adaptation in human visual cortex. J. Neurophysiol. 94, 4188–4195.
Fries, W., 1984. Cortical projections to the superior colliculus in the macaque monkey: a retrograde study using horseradish peroxidase. J. Comp. Neurol. 230, 55–76.
Genç, E., Schölvinck, M. L., Bergmann, J., Singer, W., Kohler, A. 2015. Functional connectivity patterns of visual cortex reflect its anatomical organization. Cereb. Cortex, (bhv175).
Gitelman, D.R., Parrish, T.B., Friston, K.J., Mesulam, M.M., 2002. Functional anatomy of visual search: regional segregations within the frontal eye fields and effective connectivity of the superior colliculus. NeuroImage 15, 970–982.
Graybiel, A.M., 1979. Periodic-compartmental distribution of acetylcholinesterase in the superior colliculus of the human brain. Neuroscience 4, 643–650.
Grill-Spector, K., Malach, R., 2001. fMR-adaptation: a tool for studying the functional properties of human cortical neurons. Acta Psychol. 107, 293–321.
Grön, G., Wunderlich, A.P., Spitzer, M., Tomczak, R., Riepe, M.W., 2000. Brain activation during human navigation: gender-different neural networks as substrate of performance. Nat. Neurosci. 3, 404–408.
Hall, N., Colby, C., 2014. S-cone visual stimuli activate superior colliculus neurons in old world monkeys: implications for understanding blindsight. J. Cogn. Neurosci. 26, 1234–1256.
Herman, J., Krauzlis, R., 2014. Attention to color in the primate superior colliculus. J. Vis. 14, 514.
Hess, R.F., Thompson, B., Gole, G., Mullen, K.T., 2009. Deficient responses from the lateral geniculate nucleus in humans with amblyopia. Eur. J. Neurosci. 29, 1064–1070.
Hess, R.F., Thompson, B., Gole, G., Mullen, K.T., 2010. The amblyopic deficit and its relationship to geniculo-cortical processing streams. J. Neurophysiol. 104, 475–483.
Hilbig, H., Bidmon, H.J., Zilles, K., Busecke, K., 1999. Neuronal and glial structures of the superficial layers of the human superior colliculus. Anat. Embryol. 200, 103–115.
Kaplan, E., Shapley, R.M., 1982. X and Y cells in the lateral geniculate nucleus of macaque monkeys. J. Physiol. 330, 125–143.
Kastner, S., O'Connor, D.H., Fukui, M.M., Fehd, H.M., Herwig, U., Pinsk, M.A., 2004. Functional imaging of the human lateral geniculate nucleus and pulvinar. J. Neurophysiol. 91, 438–448.
Katyal, S., Zughni, S., Greene, C., Ress, D., 2010. Topography of covert visual attention in human superior colliculus. J. Neurophysiol. 104, 3074–3083.
Kim, K.J., Rieke, F., 2001. Temporal contrast adaptation in the input and output signals of salamander retinal ganglion cells. J. Neurosci. 21, 287–299.
Krekelberg, B., Boynton, G.M., van Wezel, R.J., 2006. Adaptation: from single cells to BOLD signals. Trends Neurosci. 29, 250–256.
Laemle, L.K.A., 1981. Golgi study of cellular morphology in the superficial layers of superior colliculus of man, Saimiri, and Macaca. J. Hirnforsch. 22, 253–263.
Lee, B.B., Pokorny, J., Smith, V.C., Martin, P.R., Valberg, A., 1990. Luminance and chromatic modulation sensitivity of macaque ganglion cells and human observers. J. Opt. Soc. Am. A 7, 2223–2236.
Leh, S.E., Mullen, K.T., Ptito, A., 2006. Absence of S-cone input in human blindsight following hemispherectomy. Eur. J. Neurosci. 24, 2954–2960.
Leh, S.E., Ptito, A., Schonwiesner, M., Chakravarty, M.M., Mullen, K.T., 2009. Blindsight mediated by an S-cone-independent collicular pathway: an fMRI study in hemispherectomized subjects. J. Cogn. Neurosci. 22, 670–682.
Lennie, P., D'Zmura, M., 1988. Mechanisms of color vision. Crit. Rev. Neurobiol. 3, 333–400.
Lennie, P., Haake, P.W., Williams, D.R., 1991. In: Landy, M.S., Movshon, J.A. (Eds.), Computational Models of Visual Processing. The MIT Press, pp. 71–82.
Ling, S., Pratte, M.S., Tong, F., 2015. Attention alters orientation processing in the human lateral geniculate nucleus. Nat. Neurosci. 18, 496–500.
Lock, T.M., Baizer, J.S., Bender, D.B., 2003. Distribution of corticotectal cells in macaque. Exp. Brain Res. 151, 455–470.
Lund, J.S., Boothe, R., 1975. Interlaminar connections and pyramidal neuron organization in the visual cortex, area 17, of the macaque monkey. J. Comp. Neurol. 159, 305–334.
Maffei, L., Fiorentini, A., Bisti, S., 1973. Neural correlate of perceptual adaptation to gratings. Science 182, 1036–1038.
Marrocco, R.T., Li, R.H., 1977. Monkey superior colliculus: properties of single cells and their afferent inputs. J. Neurophysiol. 40, 844–860.
McLelland, D., Baker, P.M., Ahmed, B., Bair, W., 2010. Neuronal responses during and after the presentation of static visual stimuli in macaque primary visual cortex. J. Neurosci. 30, 12619–12631.
Merigan, W.H., Katz, L.M., Maunsell, J.H., 1991. The effects of parvocellular lateral geniculate lesions on the acuity and contrast sensitivity of macaque monkeys. J. Neurosci. 11, 994–1001.
Michna, M.L., Mullen, K.T., 2008. The contribution of color to global motion processing. J. Vis. 8, 1–12.
Movshon, J.A., Lennie, P., 1979. Pattern-selective adaptation in visual cortical neurones. Nature 278, 850–852.
Mullen, K.T., 1985. The contrast sensitivity of human colour vision to red–green and blue–yellow chromatic gratings. J. Physiol. 359, 381–400.
Mullen, K.T., Chang, D.H.F., Hess, R.F., 2015. The selectivity of responses to red-green color and achromatic contrast in the human visual cortex: an fMRI adaptation study. Eur. J. Neurosci. 42 (11), 2923–2933.
Mullen, K.T., Dumoulin, S.O., Hess, R.F., 2008. Color responses of the human lateral geniculate nucleus: selective amplification of S-cone signals between the lateral geniculate nucleus and primary visual cortex measured with high-field fMRI. Eur. J. Neurosci. 28, 1911–1923.
Mullen, K.T., Dumoulin, S.O., McMahon, K.L., de Zubicaray, G.I., Hess, R.F., 2007. Selectivity of human retinotopic visual cortex to S-cone-opponent, L/M-cone-opponent and achromatic stimulation. Eur. J. Neurosci. 25, 491–502.
Mullen, K.T., Thompson, B., Hess, R.F., 2010. Responses of the human visual cortex and LGN to achromatic and chromatic temporal modulations: an fMRI study. J. Vis. 10, 1–19.
O'Connor, D.H., Fukui, M.M., Pinsk, M.A., Kastner, S., 2002. Attention modulates responses in the human lateral geniculate nucleus. Nat. Neurosci. 5 (11), 1203–1209.
Ohzawa, I., Sclar, G., Freeman, R.D., 1985. Contrast gain control in cat's visual system. J. Neurophysiol. 54, 651–667.
Pelli, D.G., 1997. The Videotoolbox software for visual psychophysics: transforming numbers into movies. Spat. Vis. 10, 437–442.
Petit, L., Beauchamp, M.S., 2003. Neural basis of visually guided head movements studied with fMRI. J. Neurophysiol. 89, 2516–2527.
Schiller, P.H., Malpeli, J.G., 1977. Properties and tectal projections of monkey retinal ganglion cells. J. Neurophysiol. 40, 428–445.
Schiller, P.H., Malpeli, J.G., Schein, S.J., 1979. Composition of geniculostriate input to superior colliculus of the rhesus monkey. J. Neurophysiol. 42, 1124–1133.
Schiller, P.H., Stryker, M., 1972. Single-unit recording and stimulation in superior colliculus of the alert rhesus monkey. J. Neurophysiol. 35, 915–924.
Schmitz, B., Kasmann-Kellner, B., Schafer, T., Krick, C.M., Gron, G., Backens, M., Reith, W., 2004. Monocular visual activation patterns in albinism as revealed by functional magnetic resonance imaging. Hum. Brain Mapp. 23, 40–52.
Schneider, K.A., Kastner, S., 2005. Visual responses of the human superior colliculus: a high-resolution functional magnetic resonance imaging study. J. Neurophysiol. 94, 2491–2503.
Schneider, K.A., 2011. Subcortical mechanisms of feature-based attention. J. Neurosci. 31 (23), 8643–8653.
Sclar, G., Lennie, P., DePriest, D.D., 1989. Contrast adaptation in striate cortex of macaque. Vis. Res. 29, 747–755.
Sherman, S.M., Guillery, R.W., 2002. The role of the thalamus in the flow of information to the cortex. Philos. Trans. R. Soc. Lond. B 357, 1695–1708.
Sherman, S.M., Guillery, R.W., 2011. Distinct functions for direct and transthalamic corticocortical connections. J. Neurophysiol. 106 (3), 1068–1077.
Sherman, S.M., 2016. Thalamus plays a central role in ongoing cortical functioning. Nat. Neurosci. 19 (4), 533–541.
Shou, T., Li, X., Zhou, Y., Hu, B., 1996. Adaptation of visually evoked responses of relay cells in the dorsal lateral geniculate nucleus of the cat following prolonged exposure to drifting gratings. Vis. Neurosci. 13, 605–613.
Sillito, A.M., Jones, H.E., Gerstein, G.L., West, D.C., 1994. Feature-linked synchronization of thalamic relay cell firing induced by feedback from the visual cortex. Nature 369, 479–482.
Smirnakis, S.M., Berry, M.J., Warland, D.K., Bialek, W., Meister, M., 1997. Adaptation of retinal processing to image contrast and spatial scale. Nature 386, 69–73.
Smith, A.T., Cotton, P.L., Bruno, A., Moutslana, C., 2009. Dissociating vision and visual attention in the human pulvinar. J. Neurophysiol. 101, 917–925.
Solomon, S.G., White, A.J., Martin, P.R., 1999. Temporal contrast sensitivity in the lateral geniculate nucleus of a New World monkey, the marmoset *Callithrix jacchus*. J. Physiol. 517, 907–917.
Solomon, S.G., Peirce, J.W., Dhruv, N.T., Lennie, P., 2004. Profound contrast adaptation early in the visual pathway. Neuron 42, 155–162.
Sommer, M.A., Wurtz, R.H., 2004. What the brain stem tells the frontal cortex. I. Oculomotor signals sent from superior colliculus to frontal eye field via mediodorsal thalamus. J. Neurophysiol. 91, 1381–1402.
Stoerig, P., Cowey, A., 1989. Wavelength sensitivity in blindsight. Nature 342, 916–918.
Tailby, C., Cheong, S.K., Pietersen, A.N., Solomon, S.G., Martin, P.R., 2012. Colour and pattern selectivity of receptive fields in superior colliculus of marmoset monkeys. J. Physiol. 590, 4061–4077.
Talairach, J., Tournoux, P., 1988. Co-planar Stereotaxic Atlas of the Human Brain. Thieme, New York.
Tardif, E., Clarke, S., 2002. Commissural connections of human superior colliculus. Neuroscience 111, 363–372.
Vaughan, J.T., Adriany, G., Garwood, M., Yacoub, E., Duong, T., DelaBarre, L., Andersen, P., Ugurbil, K., 2002. Detunable transverse electromagnetic (TEM) volume coil for high-field NMR. Magn. Reson. Med. 47, 990–1000.
Wall, M.B., Walker, R., Smith, A.T., 2009. Functional imaging of the human superior colliculus: an optimised approach. NeuroImage 47, 1620–1627.
White, B.J., Boehnke, S.E., Marino, R.A., Itti, L., Munoz, D.P., 2009. Color-related signals in the primate superior colliculus. J. Neurosci. 29, 12159–12166.
White, B.J., Kerzel, D., Gegenfurtner, K.R., 2006. Visually guided movements to color targets. Exp. Brain Res. 175, 110–126.
Wiser, A.K., Callaway, E.M., 1996. Contributions of individual layer 6 pyramidal neurons to local circuitry in macaque primary visual cortex. J. Neurosci. 16, 2724–2739.
Zhang, P., Zhou, H., Wen, W., He, S., 2015. Layer-specific response properties of the human lateral geniculate nucleus and superior colliculus. NeuroImage 111, 159–166.